Unbalanced Harmonic Suppression of Three-Level Active Power Filter with Optimal Hybrid Control

Abstract—**Aiming at the increasingly serious harmonic pollution in power system, this paper proposes an optimized harmonic suppression strategy by combining properties of the predictive current control strategy and specific order harmonic suppression algorithm based on active power filter (APF) in a medium-voltage application occasion. Compared with the traditional harmonic suppression algorithm, the proposed algorithm not only realizes the effective compensation from low order harmonics to high order harmonics, but also compensates some specific order harmonics. In addition, the proposed strategy can achieve separation of the negative sequence part from the load current and then compensate it separately under the unbalanced condition. Finally, some experimental results are conducted to verify the correctness and reliability of the proposed algorithm based on a small-scale prototype.**

Keywords—APF, specific order harmonic control strategy, predictive current control strategy, unbalance condition, individual sequence control strategy.

I. INTRODUCTION

The demand of high-capacity active power filter in medium- and high- voltage application occasion has been found increasing due to the aggravation of harmonic problem in power system and the increasing requirement of power quality. Several harmonic suppression strategies are focused on. The harmonic detection and control strategies can be divided into two kinds: total harmonic compensation and specific order harmonic compensation. The former enables APF to compensate all harmonic currents in theory, and the latter can be used to compensate the specific order harmonic in the load current. However, the compensation capability of the above methods is still insufficient [1]-[2].

In this paper, an optimal hybrid multi-level APF control strategy is adopted, which synthesizes the properties of the specific order harmonic control strategy, predictive current control strategy and individual sequence control strategy. The experimental results verify the effectiveness and feasibility of the proposed control strategy.

II. TOPOLOGY AND MATHEMATICAL MODEL OF APF

The topology of three-level three-phase APF is shown in Fig. 1. Where, u_{sa}, u_{sb}, u_{sc} and u_{ca}, u_{cb}, u_{cc} are respectively three-phase voltages at ac source and output voltages of APF; i_{sa}, i_{sb}, i_{sc}, i_{la}, i_{lb}, i_{lc} and i_{ca}, i_{cb}, i_{cc} are respectively three-phase currents at ac source, load currents and output currents of APF. L and R are the output equivalent inductance and resistance.

According to KVL and d-q coordinate transformer [3], we get:

$$\begin{cases} u_{sa} - L\dfrac{di_{ca}}{dt} - Ri_{ca} - u_{ca} = 0 \\ u_{sb} - L\dfrac{di_{cb}}{dt} - Ri_{cb} - u_{cb} = 0 \\ u_{sc} - L\dfrac{di_{cc}}{dt} - Ri_{cc} - u_{cc} = 0 \end{cases} \tag{1}$$

$$u_{dq} = \begin{bmatrix} u_d \\ u_q \end{bmatrix} = \begin{bmatrix} -L\dfrac{di_d}{dt} + \omega L i_q - Ri_d + u_{sd} \\ -L\dfrac{di_q}{dt} - \omega L i_d - Ri_q + u_{sq} \end{bmatrix} \tag{2}$$

where, u_d, u_q and u_{sd}, u_{sq} are respectively dc components of output voltages, and the d-q channel components at ac source. i_d, i_q are respectively d- and q-channel components of output currents.

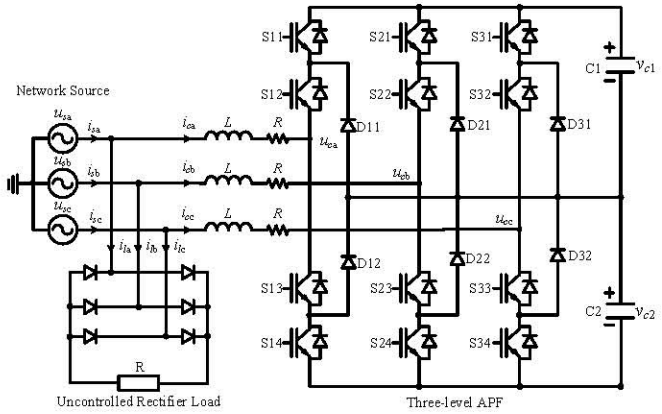

Fig. 1. The topology of three-level three-phase APF

III. The Proposed Control Strategies

A. Specific order harmonic current control strategy

The specific order harmonic detection algorithm proposed in this paper is mainly based on the d-q detection algorithm[4]-[5]. The current is subjected to d-q transformation at m times fundamental frequency by the transformation matrix of (3). The transformed dq DC component is low-pass filtered to obtain the dq component of the m-th harmonic current, thereby realizing the detection of the specific order harmonic.

$$P_m=\frac{2}{3}\begin{bmatrix}\sin m(\omega t) & \sin\left[m(\omega t-\frac{2\pi}{3})\right] & \sin\left[m(\omega t+\frac{2\pi}{3})\right]\\ -\cos m(\omega t) & -\cos\left[m(\omega t-\frac{2\pi}{3})\right] & -\cos\left[m(\omega t+\frac{2\pi}{3})\right]\end{bmatrix} \tag{3}$$

The expression of three-phase load currents is depicted as:

$$\begin{cases} i_{la}=\sqrt{2}\sum_{n=1}^{\infty}\left[I_{n+}\sin(n\omega t+\theta_{n+})+I_{n-}\sin(n\omega t+\theta_{n-})\right]\\ i_{lb}=\sqrt{2}\sum_{n=1}^{\infty}\left[I_{n+}\sin(n\omega t-\frac{2\pi}{3}+\theta_{n+})+I_{n-}\sin(n\omega t-\frac{2\pi}{3}+\theta_{n-})\right]\\ i_{lc}=\sqrt{2}\sum_{n=1}^{\infty}\left[I_{n+}\sin(n\omega t+\frac{2\pi}{3}+\theta_{n+})+I_{n-}\sin(n\omega t+\frac{2\pi}{3}+\theta_{n-})\right]\end{cases} \tag{4}$$

where, I_{n+} and I_{n-} are respectively positive and negative sequence component of the n-th harmonic; θ_{n+} and θ_{n-} are respectively initial phase angle of the positive and negative sequence component of the n-th harmonic.

Then Conducting d-q coordinate transformation based on m times fundamental-frequency current, three-phase load currents can be converted to its dc form in d-q coordinate. It is:

$$\begin{bmatrix}i_{ld}\\ i_{lq}\end{bmatrix}=P_m\begin{bmatrix}i_{la}\\ i_{lb}\\ i_{lc}\end{bmatrix}=\begin{bmatrix}\sqrt{2}I_n\sum_{n=1}^{\infty}\left[\sin((n_+ +m)\omega t+\theta_{n+})+\sin((n_- -m)\omega t+\theta_{n-})\right]\\ \sqrt{2}I_n\sum_{n=1}^{\infty}\left[\cos((n_+ +m)\omega t+\theta_{n+})+\cos((n_- -m)\omega t+\theta_{n-})\right]\end{bmatrix} \tag{5}$$

According to the above analysis, if $m=6k-1(k=1,2,\ldots,\infty)$, the positive sequence harmonic component increases by m times fundamental frequency, and the negative sequence harmonic component decreases by m times fundamental frequency. When m is equal to n, the n-th harmonic will be converted to dc component. The active and reactive components of the n-harmonic current are obtained by a low-pass filter.

In order to achieve the zero steady-state error control of the error, the traditional PI controller is adopted, so the mathematical expression of the n-th harmonic PI controller can be obtained.

$$\begin{cases} f_d=K_{Pn}\left[i_{ldn}(t)-i_{dn}(t)\right]+K_{In}\int_0^t\left[i_{ldn}(t)-i_{dn}(t)\right]dt\\ f_q=K_{Pn}\left[i_{lqn}(t)-i_{qn}(t)\right]+K_{In}\int_0^t\left[i_{lqn}(t)-i_{qn}(t)\right]dt\end{cases} \tag{6}$$

Equation (6) are respectively the active and reactive component reference of the n-th harmonic in the current space.

Since the active and reactive component can be controlled separately, and the two have symmetry, so taking the active component as an example, consider the connection reactance and the equivalent resistance. At this time, the current closed-loop control block diagram is shown in Fig. 2.

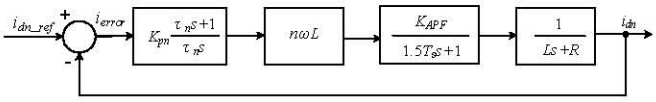

Fig. 2. n-th harmonic current closed-loop control block diagram

where $\tau=K_{pn}/K_{In}$, K_{pn} and K_{In} are respectively proportional and integral coefficients of the PI controller. T_s is sampling delay, K_{APF} is equivalent gain of APF, and $K_{APF}/(1.5T_s+1)$ is a comprehensive equivalent link of sampling delay and converter control inertial link. From this, the open-loop transfer function can be obtained:

$$H_{dn}(s)=\frac{K_{pn}K_{APF}\left(\tau_n s+1\right)n\omega L}{R(1.5T_s s+1)(1+\frac{1}{R}Ls)\tau_n s} \tag{7}$$

The APF generally requires a relatively fast current, so the PI controller parameter design can be performed according to the typical I system, and the zero point of the PI controller is used to offset the pole in the transfer function of the control object, so that:

$$H_{dn}(s)=\frac{K_{pn}K_{APF}n\omega L}{R(1.5T_s s+1)\tau_n s} \tag{8}$$

The tuning of the typical I-type system with a damping ratio of 0.707 is:

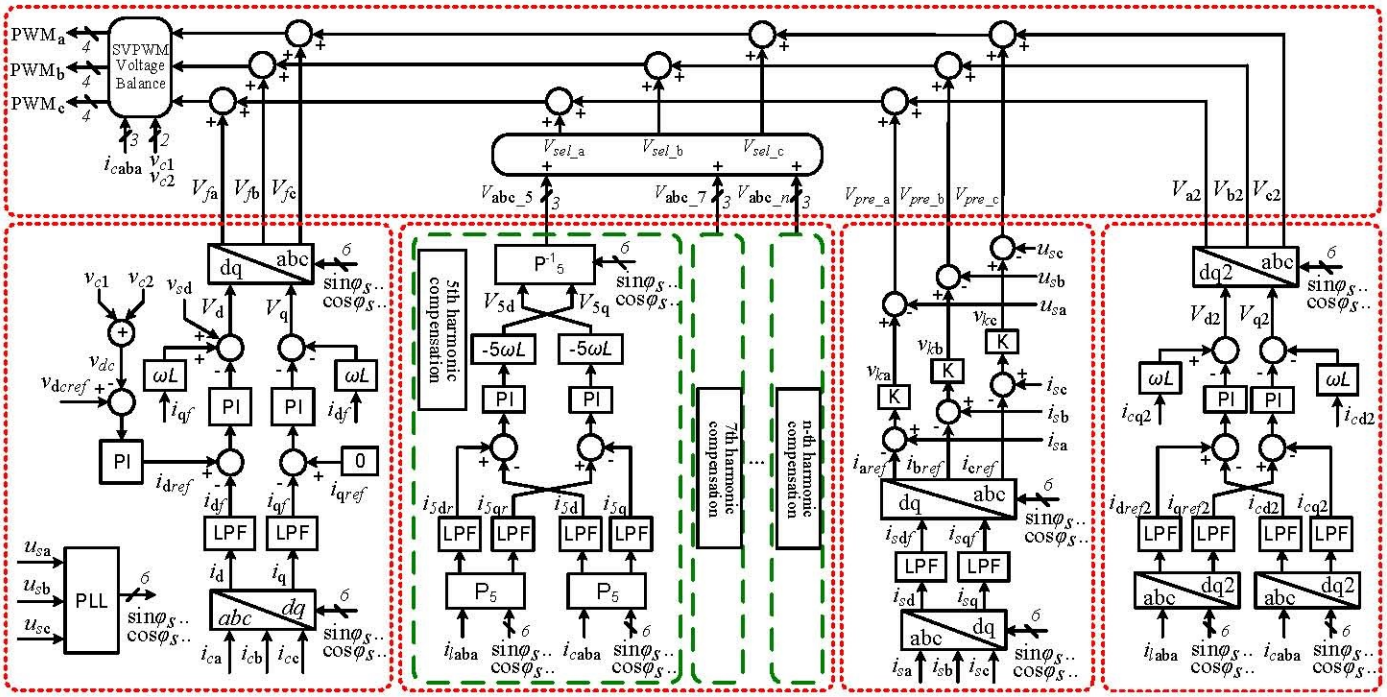

Fig. 3. Optimized active power filter overall control block diagram

$$\frac{1.5T_sK_{pn}K_{APF}n\omega L}{R\tau_n}=0.5 \tag{9}$$

So we can get the parameter calculation formula of the *n*-th harmonic current closed-loop PI controller:

$$\begin{cases} K_{pn}=\dfrac{L}{3T_sK_{APF}n\omega L} \\ K_{In}=\dfrac{K_{Pn}}{\tau_n}=\dfrac{R}{3T_sK_{APF}n\omega L} \end{cases} \tag{10}$$

In addition, the *n*-th harmonic current closed-loop transfer function is:

$$H_{cn}(s)=\frac{K_{pn}K_{APF}n\omega L}{1.5T_sR\tau_n s^2+R\tau_n s+K_{pn}K_{APF}n\omega L} \tag{11}$$

In order to make the active power filter output compensation current track the nth harmonic in the load current, when the constant $K_{pn}K_{APF}n\omega L$ is larger, the system has better dynamic performance, but if the value is too large, the stability of the system will decrease. In addition, it can be known from (11) that the PI controller parameters are affected by the harmonic order, and in the actual system, the sampling delay for each order harmonic is inconsistent. Therefore, the PI control for each order harmonic needs to be adjusted separately in order to obtain the best compensation effect.

B. *Predictive current control strategy*

The (1) can be discretized as:

$$u_{cn}(k+1)=u_{sn}(k)-L\frac{i_{cn}(k+1)-i_{cn}(k)}{T_s}-Ri_{cn}(k) \tag{12}$$

where, n = a,b,c; T_s is the sampling period. When the APF does not work, the ac current contains the harmonic current of the load, so the compensation current i_{cn} is:

$$i_{cn}(k)=i_{sfn}(k)-i_{sn}(k) \tag{13}$$

where, i_{sfn} is a fundamental component of i_{sn}. So $i_{cn}(k+1)$-$i_{cn}(k)$ can be rewritten as:

$$i_{cn}(k+1)-i_{cn}(k)=\left[i_{sfn}(k+1)-i_{sn}(k+1)\right]-\left[i_{sfn}(k)-i_{sn}(k)\right] \tag{14}$$

With higher sampling frequency, $i_{sfn}(k+1)$ and $i_{sfn}(k)$ are basically equal. So simplify (12) to:

$$i_{cn}(k+1)-i_{cn}(k)=i_{sn}(k)-i_{sn}(k+1) \tag{15}$$

Thus, after compensation by the APF, $i_{sn}(k+1)$ approximately equals to $i_{sfn}(k)$. Based on (7) and (10), we get:

$$u_{cn}(k+1)=u_{sn}(k)-K\left[i_{sn}(k)-i_{sfn}(k)\right] \tag{16}$$

where, $K = L/T_s$-R.

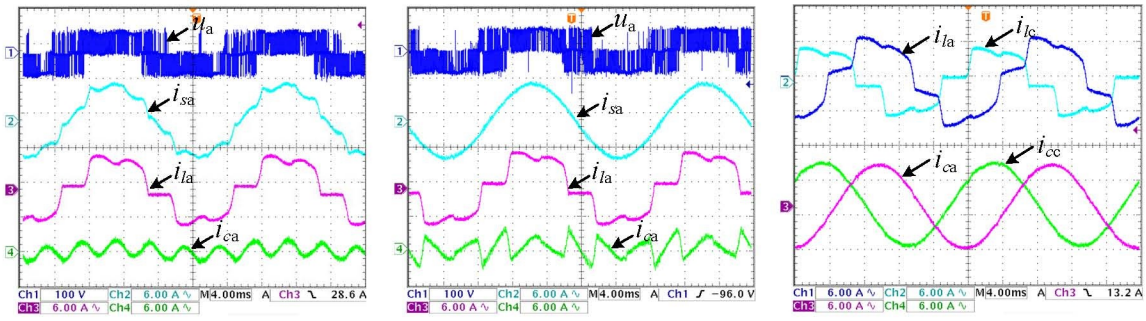

Fig. 4. APF compensation experiment results. (a) Only the fifth harmonic being compensated, (b) All order harmonics being compensated, (c) Unbalanced load being compensated

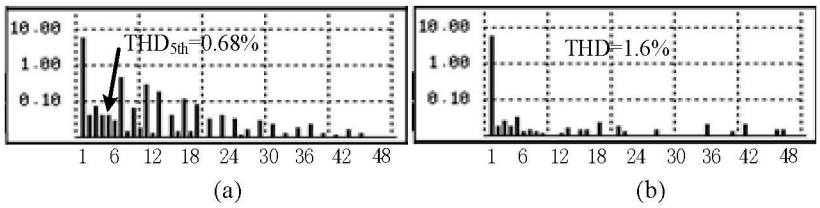

Fig. 5. Current harmonic spectrum. (a) THD after only 5th harmonic compensated, (b) Total THD spectrum

C. *Individual Sequence suppression strategy under condition of unbalanced loads*

According to the symmetrical component method [6], the asymmetric system caused by unbalanced load can be decomposed into positive sequence and negative sequence, for the three-phase three-wire system is discussed. The expressions of the unbalanced load current in the abc coordinate system and the d-q coordinate system are as follows:

$$\begin{bmatrix} i_{la} \\ i_{lb} \\ i_{lc} \end{bmatrix} = I_1 \begin{bmatrix} \sin(\omega t+\varphi_1) \\ \sin(\omega t+\varphi_1-\frac{2\pi}{3}) \\ \sin(\omega t+\varphi_1+\frac{2\pi}{3}) \end{bmatrix} + I_2 \begin{bmatrix} \sin(\omega t+\varphi_2) \\ \sin(\omega t+\varphi_2+\frac{2\pi}{3}) \\ \sin(\omega t+\varphi_2-\frac{2\pi}{3}) \end{bmatrix} \quad (17)$$

$$\begin{bmatrix} i_{ld2} \\ i_{lq2} \end{bmatrix} = I_2 \begin{bmatrix} -\cos\varphi_2 \\ \sin\varphi_2 \end{bmatrix} + I_1 \begin{bmatrix} \cos(2\omega t+\varphi_2) \\ \sin(2\omega t+\varphi_2) \end{bmatrix} \quad (18)$$

$$T_{abc-dq2} = \frac{2}{3} \times \begin{bmatrix} -\sin\omega t & -\sin(\omega t+\frac{2\pi}{3}) & -\sin(\omega t-\frac{2\pi}{3}) \\ \cos\omega t & \cos(\omega t+\frac{2\pi}{3}) & \cos(\omega t-\frac{2\pi}{3}) \end{bmatrix} \quad (19)$$

where, I_1 and I_2 are the positive-sequence and negative-sequence component amplitude of load currents respectively. In (18), the unbalanced load current can be also divided into two parts according to d-q negative sequence transformer (19), one is negative-sequence dc component, the other is a twice-frequency positive-sequence ac current component. The transformed current is passed through a low-pass filter to obtain the negative sequence component of the load current, and the block diagram is as shown.

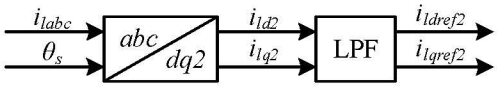

Fig. 6. Negative sequence current detection block diagram

D. *The proposed algorithm-Hybrid harmonic suppression strategy*

Based on the above control strategies, a novel harmonic optimal strategy can be obtained. it combines the properties of the specific order harmonic control, predictive current control and individual sequence suppression strategies. At the same time, a three-phase dq decoupling strategy is added to keep the DC side voltage stable. The SVPWM modulation algorithm is used to maintain v_{c1} and v_{c2} voltage balance. It can achieve a better harmonic optimal benefit and unbalance currents suppression. Its block diagram is shown in Fig.3.

IV. Experimental Result

In order to verify the correctness of the proposed strategy, a small-scaled prototype was setup. The proposed algorithm-Hybrid harmonic suppression strategy is totally coded using Verilog-HDL, synthesized using Quartus ˜ and programmed onto FPGA controller EP3C55F484C7. Three-phase AC power supply using ITECH IT7324H and the load is a three-phase uncontrolled rectifier bridge. The experimental parameters are listed as follow.

Fig.5(a) and (b) respectively show the waveforms of only the fifth harmonic, all order harmonics being compensated by the hybrid control strategy. It can be seen that the harmonics can be effectively suppressed by the proposed algorithm. The

TABLE I. EXPERIMENTAL PARAMETERS

Parameters	Values
AC line voltage	60V
Output inductance	2mH
DC voltage	130V
DC capacitor	470uF
Switching frequency	5kHz
Load	10Ω

specific results correspond to Fig.6(a) and (b), which shows 0.68% when the fifth harmonic was compensated and 1.6% when all order harmonics compensated. For the unbalanced situation, the proposed method still has a good harmonic optimal performance, as indicated in Fig.5(c).

V. CONCLUSION

This paper proposes a hybrid control strategy combined specific order harmonic control and predictive current control. Compared with traditional control methods like [7] which can only compensate for specific order harmonics separately and [8] which can only compensate for all harmonics, this proposed control method can compensate both of them, achieving better harmonic compensation effects. At the same time, the unbalanced load current is effectively suppressed by the individual sequence control strategy, so that the system can ensure better harmonic optimization characteristics under different operating conditions. Finally, the effectiveness of the proposed control strategy and good application prospects are verified by a small-scaled prototype.

ACKNOWLEDGMENT

This work was supported by Sichuan Science and Technology Program (2019JDTD0003) and Doctoral Innovation Fund Program of Southwest Jiaotong University.

REFERENCES

[1] W. Jiang, X. Ding, Y. Ni, J. Wang, L. Wang and W. Ma, "An Improved Deadbeat Control for a Three-Phase Three-Line Active Power Filter With Current-Tracking Error Compensation," in IEEE Transactions on Power Electronics, vol. 33, no. 3, pp. 2061-2072, March 2018.

[2] K. Shyu, M. Yang, Y. Chen and Y. Lin, "Model Reference Adaptive Control Design for a Shunt Active-Power-Filter System," in IEEE Transactions on Industrial Electronics, vol. 55, no. 1, pp. 97-106, Jan. 2008.

[3] B. -. Lin and T. -. Yang, "Three-level voltage-source inverter for shunt active filter," in IEE Proceedings - Electric Power Applications, vol. 151, no. 6, pp. 744-751, 7 Nov. 2004.

[4] A. Terciyanli, M. Ermis and I. Cadirci, "A Selective Harmonic Amplification Method for Reduction of kVA Rating of Current Source Converters in Shunt Active Power Filters," in IEEE Transactions on Power Delivery, vol. 26, no. 1, pp. 65-78, Jan. 2011.

[5] Z. Shu, H. Lin, Z. Ziwei, X. Yin and Q. Zhou, "Specific order harmonics compensation algorithm and digital implementation for multi-level active power filter," in IET Power Electronics, vol. 10, no. 5, pp. 525-535, 21 4 2017.

[6] X. Pei, W. Zhou and Y. Kang, "Analysis and Calculation of DC-Link Current and Voltage Ripples for Three-Phase Inverter With Unbalanced Load," in IEEE Transactions on Power Electronics, vol. 30, no. 10, pp. 5401-5412, Oct. 2015.

[7] F. Briz, P. García, M. W. Degner, D. Díaz-Reigosa and J. M. Guerrero, "Dynamic Behavior of Current Controllers for Selective Harmonic Compensation in Three-Phase Active Power Filters," in IEEE Transactions on Industry Applications, vol. 49, no. 3, pp. 1411-1420, May-June 2013.

[8] Z. Shu, M. Liu, L. Zhao, S. Song, Q. Zhou and X. He, "Predictive Harmonic Control and Its Optimal Digital Implementation for MMC-Based Active Power Filter," in IEEE Transactions on Industrial Electronics, vol. 63, no. 8, pp. 5244-5254, Aug. 2016.